Transactions on Electrical and Electronic Materials (2019) 20:420–425
https://doi.org/10.1007/s42341-019-00132-8

Online ISSN 2092-7592
Print ISSN 1229-7607

REGULAR PAPER

Photobiomodulation Therapy in Mice with Chronic Cerebral Hypoperfusion Using Application-Specific Near-Infrared Light-Emitting Diode System

Dong-Jin Lee[1] · Ha-Young Jang[3] · Ki-Wook Moon[4] · Eun-Joo Lee[3] · A-Ram Yoo[3] · Woo Sung Choi[5] · Chang Kyu Sung[4] · Dae Yu Kim[1,2]

Received: 3 June 2019 / Revised: 22 July 2019 / Accepted: 30 July 2019 / Published online: 6 August 2019

Abstract
The effective delivery of light energy from the light source to the subject is essential for an increase of therapeutic usefulness in the photobiomodulation therapy. Here, we demonstrate the application-specific near-infrared (NIR) LED therapy system applicable to the mouse for brain repair. The proposed NIR LED therapy system especially employ the curved-shape NIR LED module and the LED dimmer for optimal transfer of the light energy to the mouse brain. The therapeutic effects are evaluated in mice with chronic cerebral hypoperfusion by the positron emission tomographic scans. In the near future, we would like to quantitatively validate the therapeutic effect of our proposed NIR LED therapy system on mice with brain injury and apply it to a human brain.

Keywords Photobiomodulation · Application-specific NIR LED therapy system · Near-infrared light · Mouse with vascular dementia · Positron emission tomography

1 Introduction

The Photobiomodulation (PBM) employ a red or near-infrared (NIR) light to provide the therapeutic treatments with the functions of stimulation of healing, protection of tissue from dying, increase of mitochondrial function, and improvement blood flow and tissue oxygenation [1, 2]. The PBM can also conduct to repair the brain injury in cases of traumatic brain injury (TBI) and stroke by stimulating neurological function, increasing memory and learning capacity, and reducing inflammation and cell death in the brain [3-16]. The red and NIR light can penetrate the scalp and skull of the brain, and the transmitted photons are absorbed in two different mechanisms according to the wavelength. Cytochrome c oxidase (CCO), which is a complex protein functioning as unit IV in the mitochondrial respiratory chain, primarily absorb the photons with wavelength range of 600–940 nm and activate the nitric oxide (NO). The photons with wavelengths of 980 and 1064 nm are absorbed by transient receptor potential (TRP) calcium channels. In both ways, the absorbed photons upregulate the cell signaling and messenger molecules including reactive oxygen species (ROS) and adenosine triphosphate (ATP), which lead to activate the transcription factors such as NF-kB and blah. These transcription factors can drive the increase of gene expression linked to protein synthesis, cell migration and proliferation, anti-inflammatory signaling, anti-apoptotic proteins, and antioxidant enzymes [17, 18].

Traditionally, lasers have been widely used as light sources for PBM therapy. Lasers utilize the physical phenomenon of stimulated emission to create a monochromatic and coherent beam of light with low divergence angle. During the first 40 years of PBM research, lasers remained by far the most commonly employed light sources. It is because

✉ Dae Yu Kim
dyukim@inha.ac.kr

1 Inha Research Institute for Aerospace Medicine, Inha University, Incheon 22212, Republic of Korea

2 Department of Electrical Engineering, College of Engineering, Inha University, Incheon 22212, Republic of Korea

3 Laboratory Animal Center, Osong Medical Innovation Foundation, Cheongju, Chungbuk 28160, Republic of Korea

4 Chang Healthcare Co. Ltd, Seoul 08390, Republic of Korea

5 WOOJUNGBiO Co. Ltd, Suwon, Gyeonggi 16229, Republic of Korea

of the practices that collimated, coherent, and highly monochromatic light with the possibility of high power densities were essential to the therapeutic effects [1]. However, in recent years, light-emitting diodes (LEDs) have been commonly used due to advantages of no laser safety considerations, ease of home use, ability to irradiate a large area of tissue at once, possibility of wearable devices, and much cheaper cost per mW (2 orders lower than laser) [1, 19, 20]. LEDs emit the divergent and non-coherent light beams from spontaneous emission [21, 22]. To effectively deliver the light energy to the subjects, therefore, LED sources with optimized power and shape fitted to the subject are needed.

In this paper, we developed the application-specific NIR LED therapy system for applying the mice with chronic cerebral hypoperfusion, which leads to vascular dementia. The NIR LED therapy system was composed of power controller, micro controller unit (MCU), LED controller, and NIR LED modules. The curved-shape NIR LED module and the LED dimmer were especially employed in the proposed NIR LED therapy system for optimal transfer of the source energy to the mouse brain. To induce the chronic cerebral hypoperfusion in mice, the mice were anesthetized and conducted the bilateral common carotid artery stenosis (BCAS), which operated through the exposure of the carotid arteries and then the application of microcoils (inner diameter of 0.18 mm) in the bilateral carotid arteries. After the PBM therapy with 3 times per week for 1 month, the positron emission tomography (PET) scans were acquired in the regions of interest to evaluate the variance of the cerebral blood flow in BCAS operated mice.

2 Experiments

2.1 Application-Specific NIR LED Therapy System

Application-specific NIR LED therapy system was composed of power controller, MCU, LED controller, and NIR LED modules. The peak wavelength is 810 nm, and the power densities is in the range from 300 to 600 mW/cm^2. The NIR LED modules were made a curved shape fitted to the mouse head and placed on the top of the mouse head. The mice received treatment from the NIR LED source with constant light intensities for 30 min for 3 times per week for one month.

2.2 Animals

This study used the adult male C57BL/6 mice of 8 weeks from birth and with weight of 22–26 g. The mice were housed at one mouse per cage and were maintained on a 12-hour light/dark cycle with free access to food and water. The mice were adjusted to these conditions for 1–2 weeks prior to the experiments. The mice were assigned to the following four groups of 4–5 mice per group: a Normal group (without BCAS operation and NIR LED treatment), a BCAS group (with BCAS operation and without NIR/white LED treatment), a BCAS/NIR group (with BCAS operation and NIR LED treatment), or a BCAS/white group (with BCAS operation and white LED treatment).

2.3 Experimental Model of BCAS

8 weeks of age mice were used in the experiment. Bilateral carotid artery stenosis (BCAS) induced the chronic cerebral hypoperfusion as previously described in Ref. [23]. Briefly, mice were anesthetized using the combination of zoletil (30 mg/kg) and xylazine (10 mg/kg) via intraperitoneal injection. The carotid arteries were exposed and microcoils (inner diameter of 0.18 mm) were applied in the bilateral carotid arteries.

2.4 Positron Emission Tomography

All positron emission tomography (PET) scans were acquired using a Mediso nanoscan PET/CT (PET/SPECT-CT, Mediso Ltd., Budapest, Hungary). After injection of ^{18}F-Fluorodeoxyglucose (^{18}F-FDG) through the tail vein, the temporal change of ^{18}F-FDG uptake was monitored during first 5 min and between 45 and 90 min of PET scan. The mice were kept in the scanner under anesthesia between scans. The standardized uptake value ratio (SUVr) was obtained using the decay-corrected amount in injected ^{18}F-FDG and the weight the mouse into account.

3 Results and Discussion

Figure 1 shows the schematic representations of the application-specific NIR LED therapy system applied to the mouse with chronic cerebral hypoperfusion and primary mechanism of the PBM therapy. Each mouse was placed inside a plastic restrainer and the NIR LED module with curved shape was attached on the mouse head as shown in Fig. 1a. The emitted photons from the NIR LED module penetrate the scalp and skull of the brain, and CCO in the mitochondrial respiratory chain absorbs the NIR light with a wavelength of 810 nm as shown in Fig. 1b. The absorbed photons activate the NO and upregulate the ROS and ATP leading to activate the NF-κB and AP-1 as transcription factors causing the gene transcription linked to cell proliferation for synthesis of DNA and RNA.

Figure 2 shows the block diagram for application-specific NIR LED therapy system. The NIR LED therapy system was composed of power controller, MCU, LED controller, and NIR LED modules. The power was charged from Li-ion

polymer battery. The LED dimmer was used for control the delivered LED power.

Figure 3 shows the spectrum of emitted light from the NIR LED module and the dependence of the power densities on the distance between the NIR LED module and the mouse head. The peak wavelength of the NIR LED module was 810 nm as shown in Fig. 3a. The power density was exponentially decreased according to the distance (NIR LED

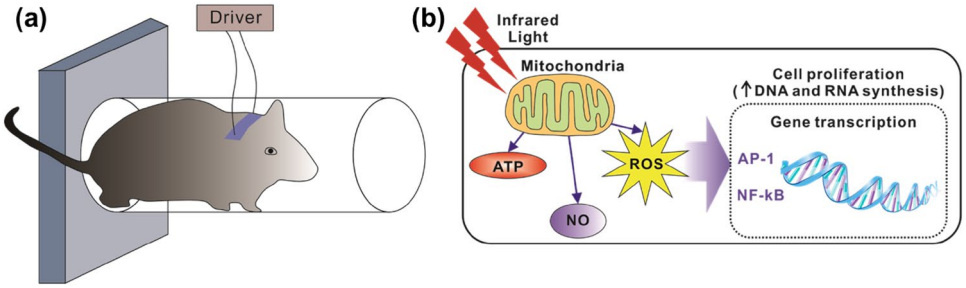

Fig. 1 Schematic representation of the application-specific NIR LED therapy system applied to the mouse with chronic cerebral hypoperfusion and dominant mechanism of the PBM therapy. **a** The mouse was placed inside a plastic restrainer and the NIR LED module with curved shape was attached on the mouse head. **b** The photons with wavelength of 810 nm can penetrate the scalp and skull of the brain, and absorbed in the CCO in the mitochondrial respiratory chain. The absorbed photons upregulate the NO, ROS, and ATP involved in the activation of NF-κB and AP-1

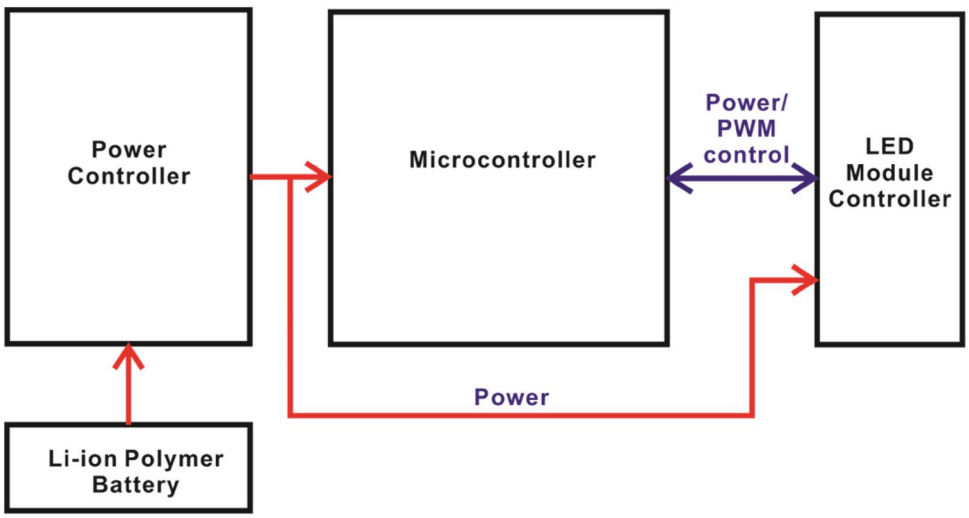

Fig. 2 Block diagram of application-specific NIR LED therapy system

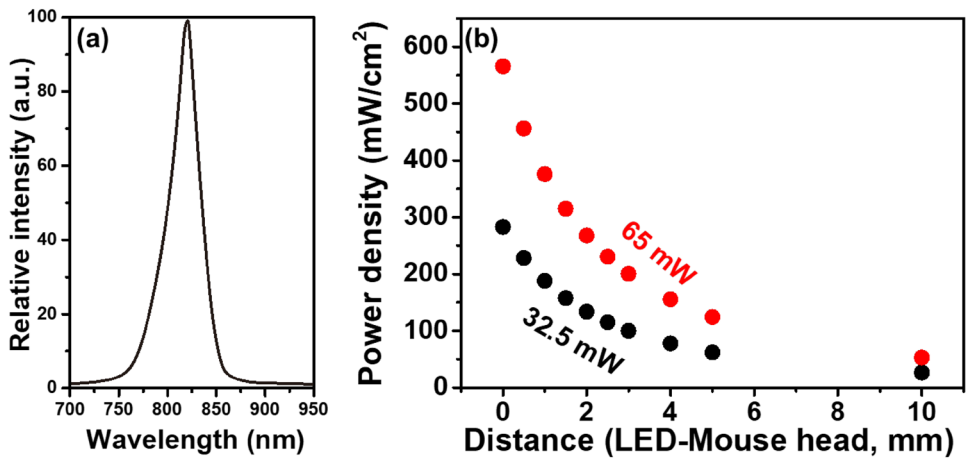

Fig. 3 The spectrum of emitted light from NIR LED module (**a**) and the dependence of the power densities on the distance between the NIR LED module and the mouse head (**b**)

module-mouse head) as shown in Fig. 3b. In this study, the NIR LED module was attached on the mouse head, so the distance between NIR LED module and mouse head was zero.

Figure 4 shows the group setting and experimental schedule for PBM therapy. The mice in this study were divided in four groups for comprehensive analysis of LED treatment: a Normal group (without BCAS operation and NIR LED treatment), a BCAS group (with BCAS operation and without NIR/white LED treatment), a BCAS/NIR group (with BCAS operation and NIR LED treatment), or a BCAS/white group (with BCAS operation and white LED treatment) as shown in Fig. 4a. Figure 4b shows the experimental schedule. The PBM therapy was perform for 1 month after 1 week of BCAS operation.

Figure 5 shows the photographic images of the PBM therapy in the mouse. The mouse was placed inside the plastic restrainer, and the NIR LED module with curved shape

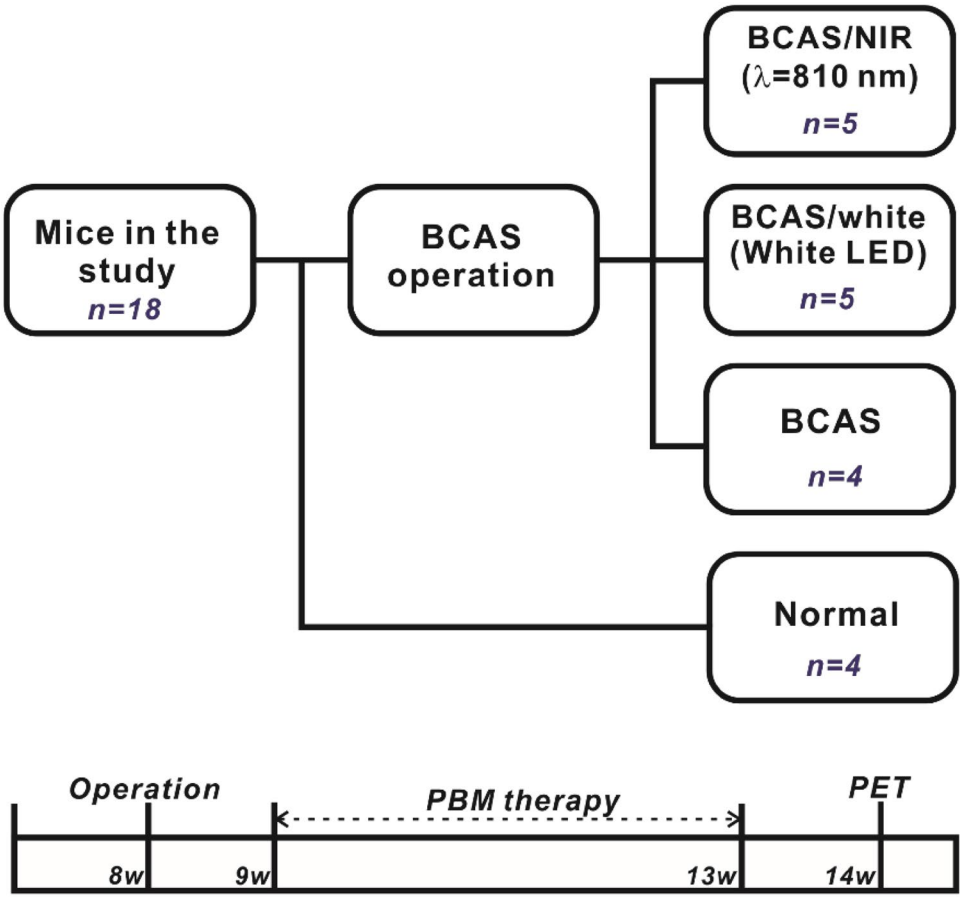

Fig. 4 Assignment of groups and experimental schedule

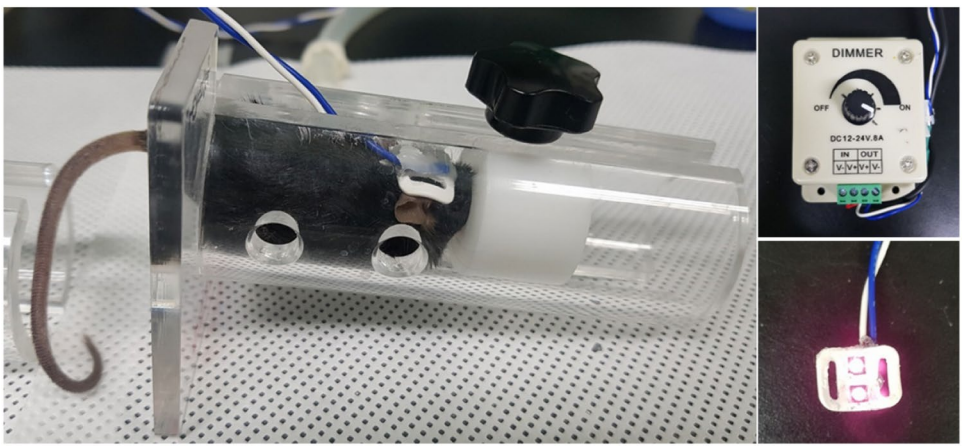

Fig. 5 Photographic images of the PBM therapy for the mouse placed inside the plastic restrainer (left), the LED dimmer (upper-right corner), and the NIR LED sources integrated in NIR LED module (lower-right corner)

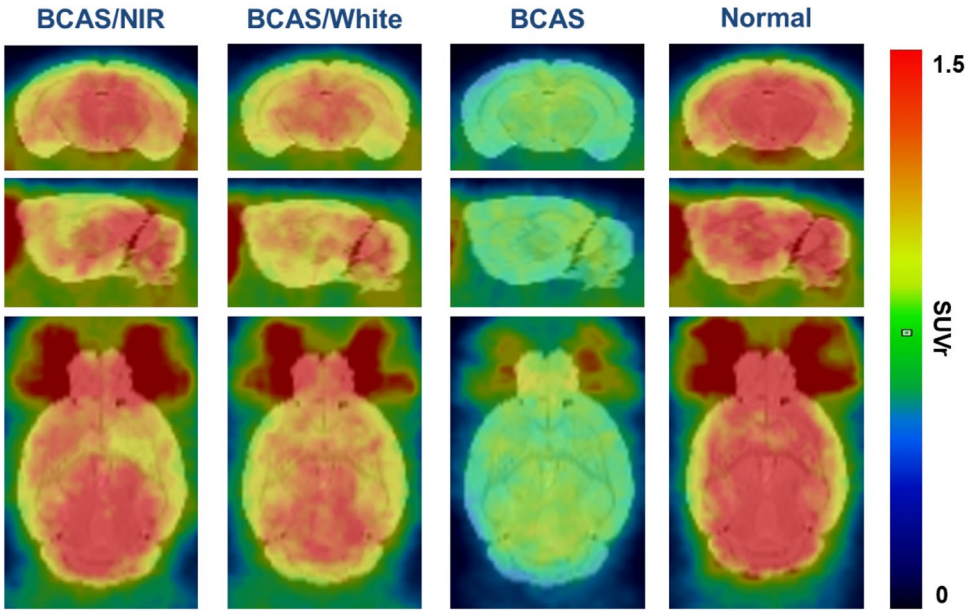

Fig. 6 The summed ^{18}F-FDG PET images in the coronal plane obtained from the 0–5 min of the scans of in the BCAS/NIR, BCAS/white, BCAS, and Normal groups. The images are superimposed on a standard MRI atlas

was attached on to the mouse head to efficiently deliver the source energy from the NIR LED module. The LED power was controlled by dimmer in the range between 300 and 600 mW/cm^2.

Figure 6 shows the summed ^{18}F-FDG PET images in the coronal plane obtained from the 0 to 5 min of the scans of in the BCAS/NIR, BCAS/white, BCAS, and Normal groups. The images are superimposed on a standard MRI atlas. The standardized uptake value (SUV) is a dimensionless ratio of predicting activity of PET imaging and mathematically defined as the ratio of radioactivity per unit volume of a region of interest (ROI) at a certain time point and the radioactivity per unit whole body volume [24]. The SUVr is also defined as the ratio of the SUV from two different regions within the same PET image: $SUVr = \frac{SUV_{target}}{SUV_{reference}}$. The SUVr of the BCAS/NIR and the BCAS/white group is higher than that of BCAS group, indicating that the cerebral blood flow is nearly recovered to normal level after LED treatment.

4 Conclusions

The application-specific NIR LED therapy system applicable to the mouse with chronic cerebral hypoperfusion induced by BCAS operation was presented. The proposed NIR LED therapy system especially employed the curved-shape NIR LED module and the LED dimmer for optimal transfer of light energy to mouse brain. To evaluate the effect of the PBM therapy in our proposed application-specific NIR LED system, the mice were divided four groups: a Normal group (without BCAS operation and NIR LED treatment), a BCAS group (with BCAS operation and without NIR/white LED treatment), a BCAS/NIR group (with BCAS operation and NIR LED treatment), or a BCAS/white group (with BCAS operation and white LED treatment). From the PET scans after the PBM therapy, we observed that the cerebral blood flow was recovered to normal level. In the near future, we would like to quantitatively validate the therapeutic effect of our proposed NIR LED therapy system on mice with brain injury and apply it to a human brain.

Acknowledgements This research was supported in part by Osong Medical Innovation Foundation through the Korea Health Industry Development Institute funded by the Ministry of Health and Welfare, Republic of Korea (No. HO16C0003010017), and in part by the National Research of Korea (NRF) grant funded by the Korea government (MIST) (No. NRF-2019R1A2C1006814), and partially supported by Basic Science Research Program through the National Research Foundation of Korea (NRF) funded by the Ministry of Education (No. 2018R1A6A1A03025523).

References

1. V. Heiskanen, M.R. Hamblin, Photochem. Photobiol. Sci. **17**(8), 1003–1017 (2018)
2. M.R. Hamblin, J. Neurosci. Res. **97**(3), 373–373 (2019)
3. B. Gefvert, Laser Focus World **52**(5), 31–35 (2016)
4. M. Hamblin, Biol. Psychiatry **81**(10), S155–S156 (2017)
5. M.R. Hamblin, Bba Clin. **6**, 113–124 (2016)
6. N.S. Hart, M. Fitzgerald, Discov. Med. **22**(120), 147–156 (2016)
7. M. Hennessy, M.R. Hamblin, J. Opt. **19**(1), 013003 (2017)
8. S.G. Hipskind, F.L. Grover, T.R. Fort et al., Photomed. Laser Surg. **34**, 77 (2018)
9. M.A. Naeser, P.I. Martin, M.D. Ho et al., Photomed. Laser Surg. **34**(12), 610–626 (2016)
10. A. Oron, U. Oron, J.L. Chen et al., Stroke **37**(10), 2620–2624 (2006)
11. G.D.R. Poiani, A.L. Zaninotto, A.M.C. Carneiro et al., Trials **19**, 17 (2018)

12. G. Rocha, P. dos Santos, W.S. Paiva et al., Med. Dev. Evid. Res. **11**, 139–146 (2018)
13. F. Salehpour, F. Farajdokht, M. Erfani et al., Brain Res. **1682**, 36–43 (2018)
14. F. Salehpour, J. Mahmoudi, F. Kamari et al., Mol. Neurobiol. **55**(8), 6601–6636 (2018)
15. C. Thunshelle, M.R. Hamblin, Photomed. Laser Surg. **34**(12), 587–598 (2016)
16. Q.H. Wu, W.J. Xuan, T. Ando et al., Lasers Surg. Med. **44**(3), 218–226 (2012)
17. L.F. de Freitas, M.R. Hamblin, IEEE J. Sel. Top. Quant. Electron. **22**(3), 15 (2016)
18. X.Y. Yao, C.L. Liu, D.X. Feng et al., Curr. Neuropharmacol. **16**(9), 1320–1326 (2018)
19. A. Basha, D.C. Mathangi, R. Shyamala, Lasers Med. Sci. **31**(9), 1803–1809 (2016)
20. J. dos Santos, A.L.C. Zaninotto, R.A. Zangaro et al., Trials **19**, 249 (2018)
21. A. Kawan, S.-J. Yu, J.-H. Sung, Trans. Electr. Electron. Mater. **19**, 230–234 (2018)
22. S. Lim, Trans. Electr. Electron. Mater. **20**, 60–66 (2019)
23. M. Ahn, Y.R. Kim, H.N. Kim et al., Sci. Rep. **6**, 28646 (2016)
24. J.A. Thie, J. Nucl. Med. **45**(9), 1431–1434 (2004)